2015 European Control Conference (ECC)
July 15-17, 2015. Linz, Austria

Experimental study of Predictive Control strategies for optimal operation of Organic Rankine Cycle systems

Andres Hernandez[1,2], Adriano Desideri[2], Clara Ionescu[1], Sylvain Quoilin[2], Vincent Lemort[2] and Robin De Keyser[1]

***Abstract*— In this paper the performance of Model Predictive Control (MPC) and PID based strategies to optimally recover waste heat using Organic Rankine Cycle (ORC) technology is investigated. First the relationship between the evaporating temperature and the output power is experimentally evaluated, concluding that for some given heat source conditions there exists an optimal evaporating temperature which maximizes the energy production. Three different control strategies MPC and PID based are developed in order not only to maximize energy production but to ensure safety conditions in the machine. For the case of the MPC, the Extended Prediction Self-Adaptive Control (EPSAC) algorithm is considered in this study as it uses input/output models for prediction, avoiding the need of state estimators, making of it a suitable tool for industrial applications. The experimental results obtained on a 11 kWe pilot plant show that the constrained EPSAC-MPC outperforms PID based strategies, as it allows to accurately regulate the evaporating temperature with a lower control effort while keeping the superheating in a safer operating range.**

I. INTRODUCTION

A growing interest on reducing the amount of world-wide industrial energy consumption has resulted in a number of studies, revealing the great potential for technologies able to recover heat at low temperatures [1]. Among the possible solutions, Organic Rankine Cycle (ORC) systems stand out for their reliability and cost-effectiveness [2].

The highly fluctuating nature of the heat source (temperature and mass flow) makes waste heat recovery (WHR) applications a challenging task. Regarding this matter control plays a major role to enable an optimal performance of the ORC unit. Dynamic modeling is an important tool, necessary to analyze system dynamics and to test control strategies during transient and/or on-off conditions, as studied for energy conversion units and for ORC systems [3].

The main challenges for the control strategy of ORC systems are twofold: 1) Keep the cycle in a safe condition during operation and 2) maximize the net output power. Safe operation of the ORC unit is important as it allows a longer life expectancy in all components. In this concern, an accurate regulation of the superheating represents an important task for the controller. The regulator has to guarantee a minimum value of superheating in order to maximize the efficiency, and avoid the formation of liquid droplets at expander inlet that can damage the expansion machine [4]. In order to maximize the output power the evaporating pressure represents the most relevant controlled variable [5].

Concerning safety and therefore regulation of superheating several controllers have been designed, based on a supervisory predictive control [6], Predictive Functional Control (PFC) [7] or generalized predictive control (GPC) as in [8]. A clear trend in the use of advanced model-based controllers, especially Predictive Controllers is confirmed in [9] where it is shown the advantages of MPC over PID strategies to regulate superheating for varying heat source profiles. Most of these studies are restricted to guarantee safety conditions by regulating the superheating but little attention is paid to the performance of the power unit in terms of energy production.

In this study we investigate the performance of MPC and PID based strategies to optimally recover waste heat in ORC technology. Therefore, *we focus not only on safety conditions but on maximizing the net output power*. The optimal evaporating temperature is derived from a steady-state model of the system as a function of the heat source conditions. The controller's task is to follow the optimal set-point generated by the optimizer while ensuring a minimum superheating value for safely operation. The performance of the proposed strategies is experimentally evaluated on a low-capacity (11 kWe) waste heat recovery unit equipped with a single screw expander.

The paper is structured as follows. Section II introduces the architecture and main characteristics of the ORC system. Next, in section III the Extended Prediction Self-Adaptive (EPSAC) approach to MPC used in this study is briefly described. A low-order model suitable for prediction is then developed using parametric identification as described in section IV. The control structure, design and tuning of the proposed PID and MPC based strategies is described in section V, followed by the experimental results in section VI. Finally a conclusion section summarizes the main outcome of this contribution.

II. PROCESS DESCRIPTION

This section describes the architecture and main characteristics of the ORC system used for evaluating the performance of the developed control strategies.

A. Hernandez and A. Desideri acknowledge the financial support provided by the Institute for the Promotion and Innovation by Science and Technology in Flanders (IWT SBO-110006).

1 Faculty of Engineering and Architecture, Department of Electrical energy, Systems and Automation, Ghent University, Belgium. e-mail: Andres.Hernandez@UGent.be

2 Thermodynamics Laboratory, University of Liege, Belgium. e-mail: adesideri@ulg.ac.be

A. The Organic Rankine Cycle System

The system considered in this study is the pilot plant available at Ghent University campus Kortrijk (Belgium). A schematic layout of the ORC system is presented in Fig. 1, where also position of the sensors are included. The system based on a regenerative cycle and R245fa as working fluid, has a nominal power of 11 kWe. The expander is originally a single screw compressor adapted to run in expander mode. It drives an asynchronous generator connected to the electric grid through a four-quadrant inverter, which allows varying the generator rotational speed (N_{exp}). During the experiments performed in this paper, the generator rotating speed is kept constant at 3000 rpm to simulate an installation directly connected to the grid. The circulating pump (N_{pp}) is a vertical variable speed 14-stage centrifugal pump with a maximum pressure of 14 bar and 2.2 kW nominal power.

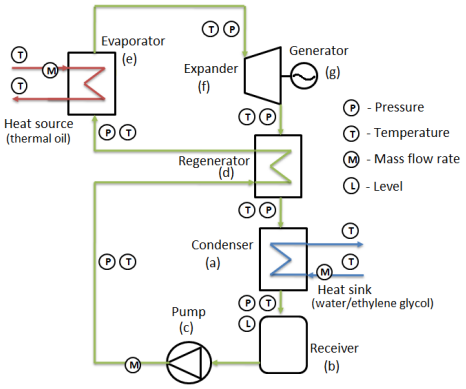

Fig. 1: Schematic layout of the pilot plant available at Ghent University, campus Kortrijk (Belgium)

Starting from the bottom of the scheme in Fig. 1, it is possible to recognize the liquid receiver (b) installed at the outlet of the condenser (a) where the fluid is collected in saturated liquid condition. From the receiver outlet, the fluid is pumped (c) through the regenerator (d) cold side, and the evaporator (e), where it is heated up to superheated vapor, reaching its maximum temperature at the evaporator outlet. The fluid, after being expanded in the volumetric machine (f), enters the regenerator hot side, and then it flows into the condenser (a) to close the cycle.

As discussed above a minimum amount of superheating at expander inlet is required to maintain safe operation. The superheating is defined as:

$$\Delta T_{sh} = T_{exp,su} - T_{sat,ev} \tag{1}$$

where $T_{exp,su}$ is the temperature measured at the inlet of the expander and $T_{sat,ev}$ the evaporating temperature, corresponding to the temperature at which the fluid undergoes the phase transition from saturated liquid to saturated vapor at the fixed evaporating pressure $P_{sat,ev}$.

$$T_{sat,ev} = f(P_{sat,ev}) \tag{2}$$

where f corresponds to a function that correlates the pressure for the refrigerant R245FA [5].

The main terms to assess the performance of the ORC system are the net output power and the cycle efficiency which are defined as:

$$\dot{W}_{el,net} = \dot{W}_{exp} - \dot{W}_{pump} \tag{3}$$

$$\eta_{cycle} = \frac{\dot{W}_{el,net}}{\dot{Q}_{in,ORC}} \tag{4}$$

where $\dot{W}_{exp}$ is the expander electrical power, $\dot{W}_{pump}$ is the pump electrical power and $\dot{Q}_{in,ORC}$ is the thermal power supplied to the ORC system in the evaporator.

B. Optimal working conditions

An experiment on the test-setup is performed to gain insight on the system's dynamics and the relationship between superheating (ΔT_{sh}), evaporating temperature ($T_{sat,ev}$), pump speed (N_{pp}) and electrical power ($W_{el,net}$) (Fig. 2).

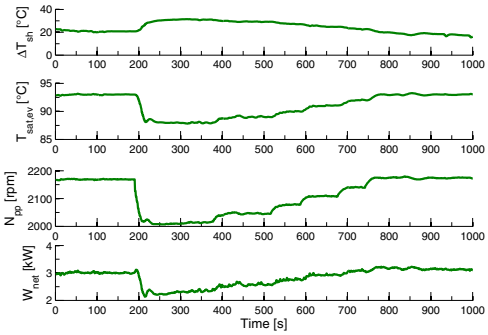

Fig. 2: Understanding the optimal operation of an ORC unit

During the entire experiment the heat source and heat sink conditions were kept constant to: $\dot{m}_{hf} = 1.3\,\mathrm{kg/s}$, $T_{hf} = 120\,^{\circ}\mathrm{C}$, $\dot{m}_{cf} = 3.8\,\mathrm{kg/s}$ and $T_{cf} = 26\,^{\circ}\mathrm{C}$. First steady-state conditions are obtained by running the pump at a constant speed of 2170 rpm. Then at time 190 s the pump speed is dropped from 2170 to 2010 rpm, resulting in a sudden decrease of the evaporating temperature and the power produced. Notice that decreasing the pump speed results on a lower mass flow of the organic fluid through the evaporator, thus decreasing the amount of thermal energy recovered, and consequently decreasing also the power generated.

Next, the pump speed is gradually increased until it reaches the same initial value of 2170 rpm, resulting in an increase of the evaporating temperature and the output power. Superheating decreases confirming that a higher efficiency has been achieved. This confirms that a low amount of superheating is desired in order to increase the efficiency of the cycle [5].

As preliminary conclusions we observe that the evaporating temperature plays an important role to maximize the output power and superheating to increase efficiency, as stated by [5], but now illustrated using real data.

C. Computing the Optimal evaporating temperature

The main conclusions obtained after analyzing the experiment are listed hereunder:

- The superheating at evaporator outlet (ΔT_{sh}) has to be maintained as low as possible, but always positive.
- The output power is strictly related to the evaporating temperature ($T_{sat,optimal}$).

The last conclusions trigger the need to define an optimal evaporating temperature, which should be adapted depending on the heat source conditions.

In this paper the optimal evaporating temperature ($T_{sat,optimal}$) is computed using an static model developed in the Equation Engineer Solver (EES). The goal is to optimize the working conditions of the cycle for a wide range of heat source conditions, while considering a constant condenser pressure, for which the following relationship is obtained:

$$T_{sat,optimal} = -88.05 + 2.44\,\dot{m}_{hf} - 0.35\,\dot{m}_{hf}^2 + 2.81\,T_{hf} - 0.011\,T_{hf}^2 \tag{5}$$

The equation (5) is valid in the range of $0.3 \leq \dot{m}_{hf} \leq 3.1\,\mathrm{kg/s}$ and $80 \leq T_{hf} \leq 145\,^{\circ}\mathrm{C}$ given a constant saturation temperature in the condenser of $p_{sat,cd} = 1.4\,\mathrm{bar}$.

In this work the control strategy is focused on accurately regulating the optimal evaporating temperature while keeping the amount of superheating above a minimum safety limit. Important to notice is that the only degree of freedom considered is the rotational speed in the pump.

III. MODEL PREDICTIVE CONTROL

MPC is a general designation for controllers that make an explicit use of a model of the plant to obtain the control signal by minimizing an objective function over a time horizon [10]. In this contribution, the Extended Prediction Self-Adaptive Control (EPSAC) proposed by [11] has been chosen as it allows to use input/output models (e.g. transfer functions), avoiding the need of state estimators.

A. Computing the Predictions

Using EPSAC algorithm, the measured process output can be represented as:

$$y(t) = x(t) + n(t) \tag{6}$$

where $x(t)$ is the model output which represents the effect of the control input $u(t)$ and $n(t)$ represents the effect of the disturbances and modeling errors, all at discrete-time index t. Model output $x(t)$ can be described by the generic system dynamic model:

$$x(t) = f\,[x(t-1), x(t-2), \ldots, u(t-1), u(t-2), \ldots] \tag{7}$$

Notice that $x(t)$ represents here the model output, not the state vector. Also important is the fact that f can be either a *linear* or a *nonlinear* function.

Furthermore, the disturbance $n(t)$ can be modeled as colored noise through a filter with the transfer function:

$$n(t) = \frac{C(q^{-1})}{D(q^{-1})} e(t) \tag{8}$$

with $e(t)$ uncorrelated (white) noise with zero-mean and C, D monic polynomials in the backward shift operator q^{-1}. The disturbance model must be designed to achieve robustness of the control loop against unmeasured disturbances and modeling errors [10].

A fundamental step in the MPC methodology consists of the prediction. Using the generic process model (6), the predicted values of the output are:

$$y(t+k|t) = x(t+k|t) + n(t+k|t) \tag{9}$$

$x(t+k|t)$ and $n(t+k|t)$ can be predicted by recursion of the process model (7) and by using filtering techniques on the noise model (8), respectively [11].

B. Optimization Procedure

A key element in linear MPC is the use of base (or free) and optimizing (or forced) response concepts [10]. In EPSAC the future response can then be expressed as:

$$y(t+k|t) = y_{base}(t+k|t) + y_{optimize}(t+k|t) \tag{10}$$

The two contributing factors have the following origin:

- $y_{base}(t+k|t)$ is the effect of the past inputs, the apriori defined future base control sequence $u_{base}(t+k|t)$ and the predicted disturbance $n(t+k|t)$.
- $y_{optimize}(t+k|t)$ is the effect of the additions $\delta u(t+k|t)$ that are optimized and added to $u_{base}(t+k|t)$, according to $\delta u(t+k|t) = u(t+k|t) - u_{base}(t+k|t)$. The effect of these additions is the discrete time convolution of $\Delta U = \{\delta u(t|t), \ldots, \delta u(t+N_u-1|t)\}$ with the impulse response coefficients of the system (G matrix), where N_u is the chosen control horizon.

The control ΔU is the solution to the following constrained optimization problem:

$$\begin{aligned} \Delta U = arg \min_{\Delta U \in \mathbb{R}^{N_u}} & \sum_{k=N_1}^{N_2} [r(t+k|t) - y(t+k|t)]^2 \\ & subject\,to\, A.\Delta U \leq B \end{aligned} \tag{11}$$

where N_1 and N_2 are the minimum and maximum prediction horizons, N_u is the control horizon, and $r(t+k|t)$ is the desired reference trajectory, here chosen as a 1^{st}-order trajectory

$$r(t+k|t) = \alpha r(t+k-1|t) + (1-\alpha) w(t+k|t)$$

for $k = 1, \ldots, N_2$ with initialization $r(t|t) = y(t)$. The signal $w(t)$ represents the setpoint and alpha (α) is a design parameter to tune the MPC performance.

The various process inputs and output constraints can all be expressed in terms of ΔU, resulting in matrices A, B [10]. As the cost function (11) is quadratic with linear constraints with respect to decision variables ΔU, then the minimization problem can be solved by a QP algorithm. In this work we make use of the Hildreth QP algorithm, to ensure numerical robustness and stability of the solution as it is particularly suitable to recover from ill-conditioned problems [12].

C. MPC tuning

In MPC, a balance between acceptable control effort and acceptable control error can be obtained via many tuning parameters (e.g. the reference trajectory design parameter α; the prediction horizon N_2 and the control horizon design parameter N_u). Closed loop performance is designed using

the N_2 parameter, whereas larger values provide a more conservative and robust control. The control horizon N_u is used to structure the future control scenario, reducing the degrees of freedom from N_2 to N_u. Structuring leads to simplified calculations and has generally a positive effect on robustness. The design parameter α in the reference trajectory can vary in the range of: $0 \leq \alpha \leq 1$. A value of α closer to 1 means a smoother variation of the setpoint and hence a less aggressive control action.

IV. Low-order Model suitable for Prediction

As mentioned above in section III, Model Predictive Control requires of a model for prediction. A trade-off between complexity of the model and prediction accuracy has to be made, in order to ensure the correct performance of the MPC strategy. In this work we have chosen a pragmatic approach by performing a parametric identification based on experimental data taken in the available setup.

The model has been identified from the manipulated variable, pump speed (N_{pp}) to the evaporating temperature ($T_{sat,ev}$) and superheating (ΔT_{sh}). The identification has been performed using a multisine excitation signal and the prediction error method (pem) [13]. The sampling time $T_s = 1$ s has been chosen according to the fastest dynamics of the system.

It is important to notice that in practice it is also possible to measure the temperature of the heat source (T_{hf}), making possible to use it as a measured disturbance. Therefore, models from this variable to evaporating temperature ($T_{sat,ev}$) and superheating (ΔT_{sh}) are also built. The nominal operating conditions of the system are presented in table I.

TABLE I: Nominal operating conditions considered for the Identification Procedure

Parameter	*Description*	*Value*	*Unit*
N_{pp}	Pump rotational speed	2000	rpm
N_{exp}	Expander rotational speed	3000	rpm
$T_{sat,ev}$	Evaporating temperature	89	$^\circ C$
ΔT_{sh}	Superheating	20	$^\circ C$
T_{hf}	Temperature hot fluid	120	$^\circ C$
$\dot{m}_{hf}$	Mass flow rate hot fluid	1.13	kg/s
T_{cf}	Temperature cold fluid	24	$^\circ C$
$\dot{m}_{cf}$	Mass flow rate cold fluid	4	kg/s
$\dot{W}_{el,net}$	Net output power	11	kW
η_{cycle}	Cycle efficiency	6	%

The identified model is presented in (12) in the form of transfer functions.

$$\begin{bmatrix} \Delta T_{sh}(s) \\ T_{sat,ev}(s) \end{bmatrix} = \begin{bmatrix} \frac{-0.117}{(20.55s+1)} \\ \frac{0.032}{(9.217s+1)} \end{bmatrix} [N_{pp}] + \begin{bmatrix} \frac{1.355}{(1.61s+1)} \\ \frac{0.031(s+0.001934)}{(s^2+0.226s+0.054)} \end{bmatrix} [T_{hf}] \quad (12)$$

The normalized root-mean-square error of each transfer function to validation data was computed using (13):

$$fit = 100 * \left(1 - \frac{\|y - \hat{y}\|}{\|y - mean(y)\|}\right) \quad (13)$$

where y is the validation data output and $\hat{y}$ is the model output given by the transfer function. Each transfer function gave a data fitting above 70%.

V. Control Structure and Tuning

In this section two group of strategies (i.e. basic and optimal) are proposed to regulate the evaporating temperature and to keep superheating in a safe range. For each of the strategies PID- and MPC-like schemes will be developed and tested as explained in the following subsections.

An important element on the control design are the physical constraints and the safety conditions of the system. For which, the controller is required to respect the following input (pump speed) and output (superheating) constraints as summarized in table II.

TABLE II: Operation constraints of the ORC unit

Variable	*max*	*min*	Δ
Pump Speed N_{pp}	2200 rpm	1800 rpm	20 rpm/s
Superheating ΔT_{sh}	–	15 °C	-

A. Basic strategies

In the basic strategies a fixed setpoint for the evaporating temperature is used $T_{sat,ref} = 90\,^\circ$C. This choice emulates the cases when the designer computes the reference for some steady-state conditions under the hypothesis that the variations of the heat source will not affect 'too much' the performance. The proposed control scheme of the ORC unit is depicted in Fig. 3.

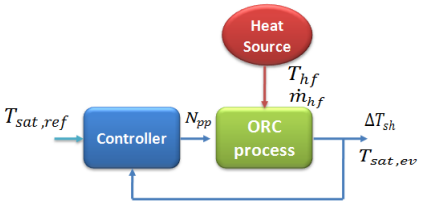

Fig. 3: Control structure for basic strategies: with fixed evaporating temperature setpoint

Basic PI: this strategy refers to the case when the controller in Fig. 3 is based on a PI. The PI controller for evaporating temperature is tuned using the transfer function which relates the speed in the pump to the evaporating temperature found in (12). The CAD tool FRTool [14] is used to tune the controller for the following design specifications: settling time $T_{set} = 100s$, overshoot percent $OS\% = 0$ and robustness $R_o = 0.7$, obtaining the following PI parameters:

$$PI_{T_{sat,ev}} = K_p \left(1 + \frac{1}{T_i s}\right) = 7.57 \left(1 + \frac{1}{4.43 s}\right) \quad (14)$$

During the implementation phase of (14) an anti-reset windup scheme is used to clip the control action into the permissible range of the pump (table II).

Basic MPC-EPSAC: in this strategy a MPC controller is used in Fig. 3, offering the possibility to include not only input but also output constraints in the optimization problem, thus ensuring a minimum superheating as requested for safety reasons (table II).

A trade-off between closed loop speed and robustness has been obtained for $N_2 = 40, N_u = 1, \alpha = 0.5$. The main goal

is to achieve a response without overshoot $OS\% = 0$ and settling time of about 100 s. Another important element in the design of the controller is the choice of the disturbance model (8), during this study the filter $C(q^{-1}) = 1, D(q^{-1}) = 1 - q^{-1}$ has been chosen leading to zero steady-state error. Notice that this filter choice acts like the integral action for PID controllers.

B. Optimal strategies

The optimal strategies make use of the optimizer (5) to generate as a function of the heat source variations the optimal setpoint to the controller, as illustrated in Fig. 4. Two strategies PID- and MPC-based are developed in order to control the ORC unit.

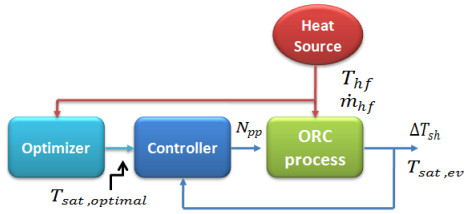

Fig. 4: Control structure for optimal strategies: optimizer computes the optimal evaporating temperature setpoint.

Switching PIs: In this strategy a PI controller is used to follow the optimal saturation temperature $T_{sat,optimal}$, until the superheating goes below a threshold value of 15 °C in which case another controller for superheating with setpoint at $\Delta T_{sh,ref} = 17$ °C will take over in order to bring the system into a safer condition. This switching mechanism is used to maximize the output power by tracking $T_{sat,optimal}$, while providing some safety for the case of superheating values below 15 °C. While the PI controller for the evaporation temperature is the same used on the basic PI strategy (14), the PI controller for superheating is tuned using the transfer function which relates the pump speed to the superheating as found in (12). Using the CAD tool FRTool [14], and the design specifications: settling time $T_{set} = 100s$, overshoot percent $OS\% = 0$ and robustness $R_o = 0.7$, the following PI parameters are obtained:

$$PI_{\Delta T_{sh}} = K_p \left(1 + \frac{1}{T_i s}\right) = -1.1 \left(1 + \frac{1}{0.98\, s}\right) \qquad (15)$$

Optimal MPC-EPSAC: in this strategy the same EPSAC controller as the basic MPC is used (i.e. $N_2 = 40, N_u = 1, \alpha = 0.5$), the only difference is the setpoint. Instead, of following a fixed setpoint, the MPC controller will track the optimal setpoint generated using the optimizer (Fig. 4). Input and output constraints are also implemented in this controller as requested on table II.

VI. EXPERIMENTAL RESULTS

An experimental campaign has been carried on, to test the different control strategies and to define which one allows to maximize the net output power given a defined trend of the thermal energy source. In this experiment the variations of the thermal energy source are due to variations of ±10 °C in T_{hf} around the nominal value of 120 °C, while other conditions were kept constant as observed in Fig. 5.

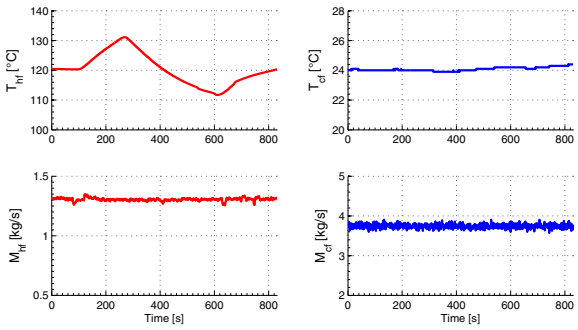

Fig. 5: Heat source (left) and heat sink conditions (right) during closed loop tests.

In Fig. 6a the results obtained for the basic strategies (i.e. fixed setpoint) are shown.

In the basic PI strategy we want the controller to keep the evaporating temperature at a constant value of 90 °C. Once the temperature of the heat source (T_{hf}) starts rising, temperature at the inlet of the expander ($T_{exp,su}$) will rise, thus resulting on higher superheating values, as expected from (1). Therefore, decreasing the efficiency of the cycle and its net output power. Regarding safety conditions, the most dangerous situation appears around time 600 s when T_{hf} decreases. Thus, resulting in a sudden drop in the superheating value, which could result on liquid drops in the expander.

For the basic MPC strategy, the setpoint for evaporating temperature is still constant, thus obtaining a suboptimal performance (i.e., high values of superheating when T_{hf} rises and therefore a low net output power). Nevertheless, since we included output constraints in the MPC formulation, superheating is always above the threshold value ($\Delta T_{sh} > 15$ °C), thus leading to a safer operation.

Subsequently, we are interested on evaluating the performance of the optimal strategies, i.e., once the optimizer is used to maximize the energy production as depicted in Fig. 6b. The switching PI mechanism avoids the superheating to decrease dramatically compared to the basic PI, nevertheless it still undergoes the threshold value by 5 °C and requires a more agressive control action. Hence, making of the basic MPC a safer and therefore more desirable strategy.

Finally, the optimal MPC strategy is tested as depicted in Fig. 6b. An important aspect to highlight in this strategy is the fact that it requires a less agressive control effort (pump speed N_{pp}) compared to the switching PI, thus resulting in a higher net output power and higher life expectancy of the actuator.

Notice that for the optimal strategies the superheating is in average lower compared to the basic strategies, thus resulting in a higher efficiency of the cycle and higher output power. The analysis of the results demonstrate that MPC outperforms the PI based strategies for the given conditions, however, it is still interesting to investigate the net output power. The resulting net output power was integrated over the time in order to calculate the energy produced for each

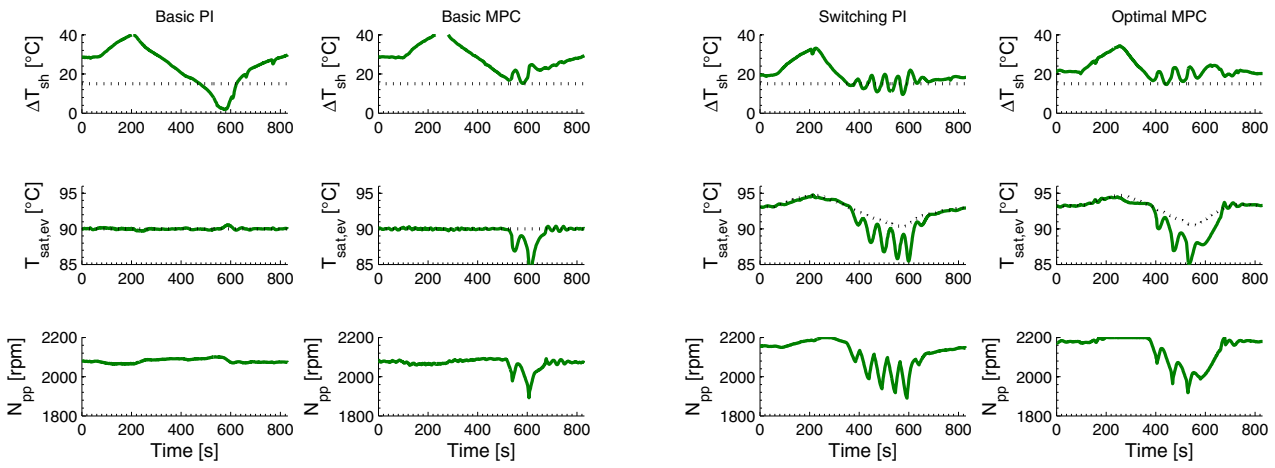

(a) Basic strategies

(b) Optimal strategies

Fig. 6: Performance of the different control strategies for a varying thermal energy source.

of the strategies as summarized in table III.

TABLE III: Control strategy performance and energy production

Controller	Energy Produced	Profit
Basic PI	Unsafe	–
Basic MPC	2.773 kWh	115 %
Switching PI	2.413 kWh	100 %
Optimal MPC	**2.915** kWh	**121** %

By taking the switching PI as reference (100%) of the net electrical energy produced, it is possible to observe that the basic MPC produces 15% more energy as it requires of a lower control effort while keeping the unit in safe operation. These results are enhanced by combining the use of an optimizer and the MPC strategy, thus resulting in an extra profit of 6% if compared to basic MPC or 21% if compared to the PI strategy based on the switching mechanism.

VII. CONCLUSIONS

In the present contribution several PID and MPC based strategies have been designed and experimentally tested, with the goal to optimize the working condition of an ORC unit for waste heat recovery applications.

The experimental results obtained in a low-capacity pilot plant show that for the case of variations in the thermal energy source, a characteristic of waste heat recovery applications, the MPC allows to produce about 21% more net electrical output power compared to classical PI based control. This is achieved by more accurately regulating the optimal evaporating temperature generated by the optimizer, while keeping the superheating at low but still safe values, resulting also in a higher efficiency of the system.

Future work includes the development of a multivariable control strategy, by considering the expander speed, the mass flow rate and/or temperature of the heat sink as possible degrees-of-freedom.

REFERENCES

[1] IEA, "Industrial excess heat recovery technologies & applications," Technical report, Industrial Energy-related Technologies and Systems (IETS), Tech. Rep., 2010.

[2] A. Verneau, "Waste heat recovery by organic fluid rankine cycle," in *In Proceedings from the First Industrial Energy Technology Conference*, Houston, TX, 1979, pp. 940–952.

[3] F. Casella, T. Mathijssen, P. Colonna, and J. Van Buijtenen., "Dynamic modeling of organic rankine cycle power systems," *Journal of Engineering for Gas Turbines and Power*, vol. Vol 135, pp. 042 310–042 310–12, 2013.

[4] D. Wei, X. Lu, Z. Lu, and J. Gu., "Performance analysis and optimization of organic rankine cycle (orc) for waste heat recovery," *J. Energy Conversion and Management*, vol. Vol. 48, pp. 1113–1119, 2007.

[5] S. Quoilin, R. Aumann, A. Grill, A. Schuster, and V. Lemort., "Dynamic modeling and optimal control strategy for waste heat recovery organic rankine cycles," *Applied Energy*, vol. Vol. 88, pp. 2183–2190, 2011.

[6] G. Hou, R. Sun, G. Hu, and J. Zhang., "Supervisory predictive control for evaporator in organic rankine cycle (orc) system for waste heat recovery," in *Proceedings of the 2011 International Conference on Advanced Mechatronics Systems*, 2011, pp. 306–311.

[7] V. Lemort, A. Zoughaib, and S. Quoilin., "Comparison of control strategies for waste heat recovery organic rankine cycle systems," *In Sustainable Thermal Energy Management in the Process Industries International Conference (SusTEM2011)*, 2011.

[8] J. Zhang, Y. Zhou, Y. Li, G. Hou, and F. Fang., "Generalized predictive control applied in waste heat recovery power plants," *Applied energy*, vol. 102, pp. 320–326, 2013.

[9] A. Hernandez, A. Desideri, C. Ionescu, S. Quoilin, V. Lemort, and R. D. Keyser., "Increasing the efficiency of organic rankine cycle technology by means of multivariable predictive control." in *Proceedings of the 19th World Congress of the International Federation of Automatic Control (IFAC 2014)*, 2014.

[10] E. F. Camacho and C. Bordons., *Model Predictive Control*, 2nd ed. Springer-Verlag, London,, 2004, vol. 405 pages.

[11] R. De Keyser, *Model based Predictive Control for Linear Systems*. Invited chapter in UNESCO EoLSS. Oxford (6.43.16.1), 2003.

[12] L. Wang, *Model Predictive Control System Design and Implementation Using MATLAB®*, ser. Advances in Industrial Control. Springer, 2010.

[13] L. Ljung, *System identification: theory for the user*. Prentice-Hall, 2007.

[14] R. De Keyser and C. Ionescu., "A frequency response tool for cacsd in matlab," in *IEEE International Symposium on Computer Aided Control Systems Design*, Munich, 2006, pp. 2275–2280.